FPGA-based Single Photon Counting and Timing from an Array of Superconducting Nanowire Single Photon Detectors

N. Lusardi, F. Garzetti, G. Bulgarini, A. Geraci

***Abstract* – Counting single photons and measuring their arrival time is of crucial importance for imaging, computing or communication applications that use single photons or few photons to outperform classical techniques. Single photons or pair of photons can for instance be used to enhance the resolution of optical imaging techniques [1], or to transmit information with ultimate security using quantum cryptography [2]. In order to maintain this performance gain in such applications, the exact number of photons and their arrival time must be measured and monitored. In this contribution, we present a method to measure the number of photons and their arrival time by using 16 Superconducting Nanowire Single Photon Detectors (SNSPDs) [3] optically coupled to a weak laser via a fiber multiplexer.**

Since a single SNSPD is not sensitive to the number of incoming photons, the optical signal multiplexing is necessary to measure photon correlations among the channels and thus reconstruct the statistics of the optical pulse. The readout and counting of the photon arrivals is performed with a fast multi-channel Asynchronous-Correlated-Digital-Counter (ACDC) [4] whereas the arrival time is measured by an high resolution multi-channel Time-to-Digital Converter (TDC) with resolution of 10 ps, full-scale-range of 640 ns and global precision guaranteed below 22 ps r.m.s. referred to each single channel [5, 6].

Both of the ACDC and the TDC are implemented in the Programmable Logic (PL) of a Xilinx Zynq®-7 XC7Z020 Xilinx System-of-Chip (SoC) device hosted in a customized acquisition board interfaced outside by means of a USB 3.0 communication gate.

I. Introduction

Extremely sensitive light sensing can be performed by observing the transition of a section of a current-biased superconducting nanowire from the superconducting state to the normal resistive state, as a result of photon absorption. Devices based on this principle are called Superconducting Nanowire Single Photon Detectors (SNSPDs) and find application in several areas of quantum information technology for their ability of detecting single photons with near unity probability in a large wavelength range from UV to infrared. SNSPDs have been used to measure single-photon emission from a wide variety of light sources as, for example, individual dopants in carbon nanotubes, color centers in silicon carbide and semiconductor quantum dots. In addition to high photon detection efficiency, SNSPDs provide several advantages in comparison to other single-photon sensitive devices: extremely low timing jitter, the absence of afterpulsing and the low dark count rate. Such performances make them the ideal detector for applications where efficient detection of weak signals with high time resolution is required. Examples includes photon correlations, high-resolution light detection and ranging (Lidar), oxygen singlet detection, optical time domain reectometry in telecommunication networks and deep-space optical communication.

In [4, 5, 6] we have presented the implementation of a resource-saving 8-channels Time-to-Digital Converter (TDC) with resolution of 10 ps and precision below 22 ps r.m.s. and an Asynchronous-Correlated Digital-Counter (ACDC) in a FPGA device for timing and correlating photon counting for SNSPDs array.

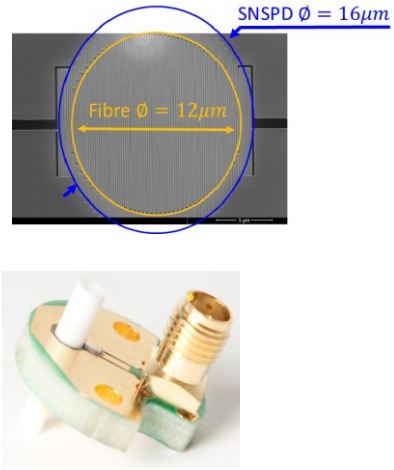

Fig. 1. Optical coupling (top) from the SNSPD (bottom) (diameter 16μm) to the optical fiber (diameter 12μm).

Manuscript received November, 10, 2017.
N. Lusardi and A. Geraci are with the Politecnico di Milano, Department of Electronics, Information and Bioengineering – DEIB, via Golgi 40, 20133 Milano MI, Italy (E-mail: nicola.lusardi@polimi.it; angelo.geraci@polimi.it).
G. Bulgarini are with Single Quantum B.V., 2628 CH Delft, The Netherlands.

II. Description of the Detector

The detector has the shape of a meandering nanowire of NbTiN with 100nm width and 50 fill factor. The nanowire detector covers an area of diameter 16µm. The superconductor is positioned on top of a resonant cavity formed by a silicon-oxide layer of 135nm and gold in order to enhance the photon absorption probability at ~800nm (Fig.1). This wavelength range is particularly important for quantum experiments since state-of-art single photon sources, based on photon down-conversion, provide photon emission in this wavelength range. The detector is operated at a temperature of ~2.5K and is coupled to a single-mode optical fiber. Fig. 2 shows the calibration of one superconducting nanowire detector used in these experiments. The system detection efficiency measured at 878nm is plotted as a function of the bias current applied to the superconducting sensor. The device reaches, at saturation, a system detection efficiency of 80.7%. This efficiency represents the ratio of the detected photon rate with respect to the photon rate at the cryostat input. It therefore includes optical losses at the fiber connector located at the cryostat input and it also includes the transmission losses of the optical fiber that connects the superconducting detectors from inside the cryostat to the cryostat input. Fig. 3 displays the measured time distance of a laser trigger from a mode-locked Ti:Sapphire laser. The distribution of detection pulses shows a timing jitter (σ_{jitter}) of 19.84ps r.m.s., which corresponds to 46.62ps FWHM for a Gaussian fit. The measurement in Fig. 3 is acquired with a LeCroy Waverunner 640Zi oscilloscope. The electrical jitter of the laser trigger signal (σ_{LASER}) has been measured separately and resulted in a contribution of less than 6ps r.m.s. corresponding to 14ps FWHM. The contribution of the oscilloscope (σ_{SCOPE} below 2ps r.m.s. that is below 4.7ps FWHM) can be neglected. The jitter contribution of the SNSPD (σ_{SNSPD}) is below 8ps r.m.s. and of the amplification stage (σ_{AMPLI}) is less than 14ps r.m.s., i.e.

$$\sigma^2_{jitter} = \sigma^2_{SNSPD} + \sigma^2_{AMPLI} + \sigma^2_{LASER} + \sigma^2_{SCOPE} \approx$$
$$\approx \sigma^2_{SNSPD} + \sigma^2_{AMPLI} + \sigma^2_{LASER}$$

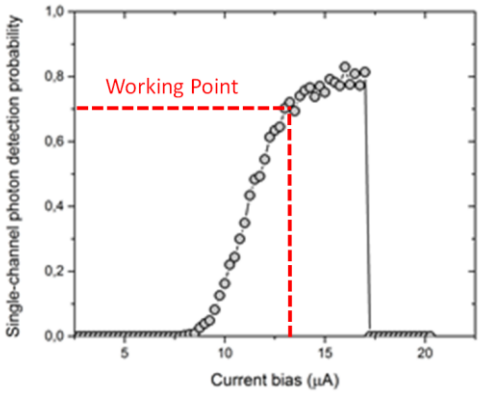

Fig. 2. Efficiency vs Current.

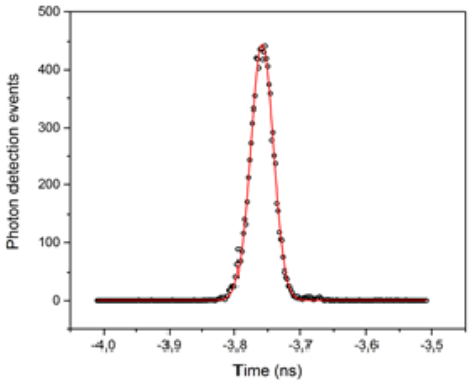

Fig. 3. Timing jitter of the amplified SNSPD.

III. Experimental Setup

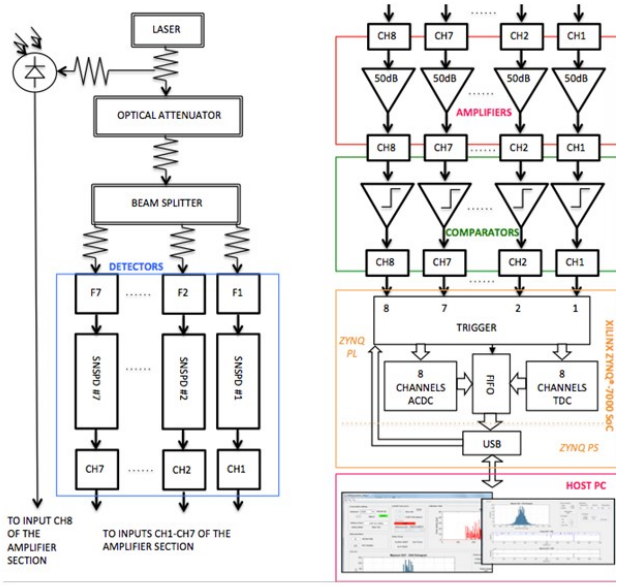

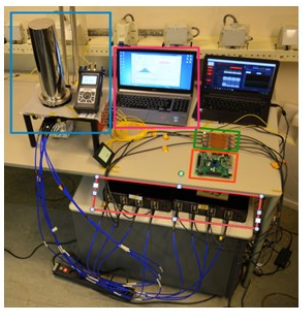

Fig. 4. Schematic description of measurement setup (top) and corresponding picture (bottom). The sub-systems of the measurement setup are highlighted with colored corresponding frames both in the schematics and in the picture.

Timing measurements and photon statistics are performed by means of a Time-to-Digital Converter (TDC) [4] and an Asynchronous-Correlated-Digital-Counter (ACDC) [5] respectively. Both the TDC and the ACDC are implemented in the Programmable Logic section (PL) of a System-on-Chip (SoC) programmable device, i.e. a Xilinx Zynq-7020 (XC7Z020-1 CLG484 33,650 SLICEs, 66,400 kbit BRAM, 400 DSPs) [7], that integrates a 28nm Xilinx's Artix-7 FPGA within the Programmable Logic (PL) section and an ARM-based processor in the Programmable Software section (PS).
The setup is composed of five different main parts (Fig. 4), which are a detection section, an analog stage, a group of comparators for digitizing the output of the analog stage, the SoC that includes TDC and ACDC and a read-out software running on a host PC. Purpose of this setup, limited to 7 SNSPDs and laser, is collect enough information and experience for creating a robust, compact and user friendly system that to acquire timing measurement and photon statistic up to 16 SNSPDs.

B. *Analog stage*

The signal at the output of each detector has a decreasing exponential shape with peak amplitude of about 0.5mV and nominal decay time constant equal to 14ns (Fig. 5). The analog stage is composed of 8 (one per channel) AC-coupled pass-band and low-noise double-stage amplifiers, with gain 50dB over the bandwidth 10MHz - 1GHz adding timing jitter (σ_{AMPLI}) <14ps r.m.s. to the intrinsic jitter of the single SNSPD that is less than 8ps r.m.s.

C. *Comparators*

Each output of the 8 analog amplifiers is converted in a digital pulse by a programmable threshold discriminator [8] based on an ultra-fast and low-jitter comparator (Analog Devices ADCMP605BCPZ [9]), whose output is a logic level in LVDS format. The timing jitter introduced by each comparator (σ_{CMP}) is below 7ps r.m.s.
A baseline fluctuation (σ_{BASE}) less than 40ps r.m.s. is introduced by the stochastic rate of arrival of the events. We restore the baseline by applying a high-pass filter at 100MHz at the input of the comparators (Fig. 6) [4].

D. *Time-to-Digital Converter*

The 8-channel TDC system is a Wave-Union-A Tapped-Delay-Line TDC (WUA-TDL-TDC) implemented in the Programmable Logic (PL) of the SoC [10, 11].
Main features of the WUA-TDL-TDC architecture (only the firmware) are the low power consumption (430mW) and the very modest expense of resources necessary for implementation (30% of the PL section). The resolution of the TDC is 8.6ps and the single channel precision is guaranteed

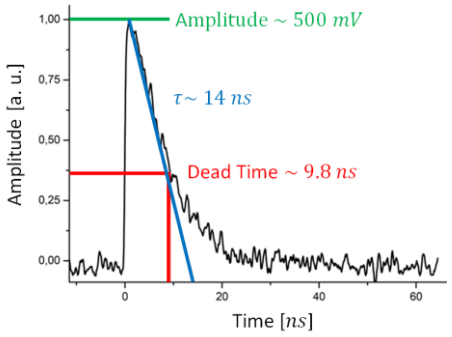

Fig. 5. Picture of the signal at the output of the SPSPD.

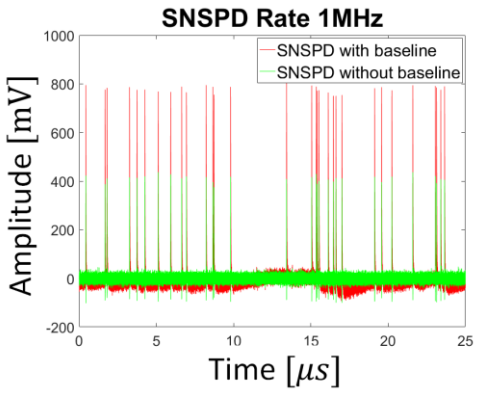

Fig. 6. Baseline fluctuation at 100MHz in amplified SNSPD (red) and the restored version (green).

TABLE I
CHARACTERISTICS OF THE IMPLEMENTED TDC

Feature	Value
Number of Channels	8
TDC clock frequency	400MHz
System frequency	100MHz
Decoding/Calibration Hardware in FPGA	1 per channel
Device Occupation per Channel	314SLICEs, 54kbit BRAM
Pipeline Latency	110ns
Maximum Channel Rate of measurement	10MHz/channel
Channel Resolution	8.6ps
TDC Channel Precision	< 15 ps r.m.s.
Full Scale Range	640ns
Channels Cross Talk	No spurious measure on idles and active channels
Precision Crosstalk Influence	< 3 ps r.m.s on active channels, nothing on idle ones

below 15ps r.m.s. per channel (σ_{TDC}); moreover, if we consider the threshold comparator as input, the channel precision is 17ps r.m.s. due to the contribution of σ_{CMP} and σ_{TDC}. The precision is kept constant over the full-scale range. The nominal full-scale-range of the WUA-TDL-TDC is 10.7 seconds, but this value is limited to 640ns because the maximum time interval under measurement is the time skew between two different channels, which is lower than few tens of ns. All the characteristic of the WUA-TDL-TDC are summarize in Tab. I.

E. Asynchronous-Correlated-Digital-Counter

The ACDC is implemented in the PL of the SoC and has 8 channels, it detects the presence of an event per channel for each single acquisition. The maximum trigger time resolution is 10ns, which is significantly smaller than the maximum rate of detection, in our experiment, due to the temporal distances of the lasers pulses (i.e. >12.6ns). One channel is set as trigger of the acquisition process and gives the start for the photon counting on the other channels within a programmable time window (Fig. 7).

F. Read-out software

The user selects via software the triggering channel and the duration of the measurement window. First, the SoC device performs the time measurements of the WUA-TDL-TDC implemented on the programmable logic, then it sends measurement data to the host PC via USB. By means of the read-out software hosted on a standard computer, the user can set which channel is the "start" of the acquisition and the duration by a programmable time window. The WUA-TDL-TDC/ACDC provides data in real-time, so the user on the host PC can perform real-time timing statistics among the 8 channels and, after the acquisition, the corresponding photon statistics.

In order to minimize the total jitter, it is worth using an acquisition time that is shorter or equal to the repetition period of the laser pulses. Consequently, the procedure involves the acquisition of the 7 channels after receiving a laser pulse that triggers the start of the measurement as shown in Fig. 7.

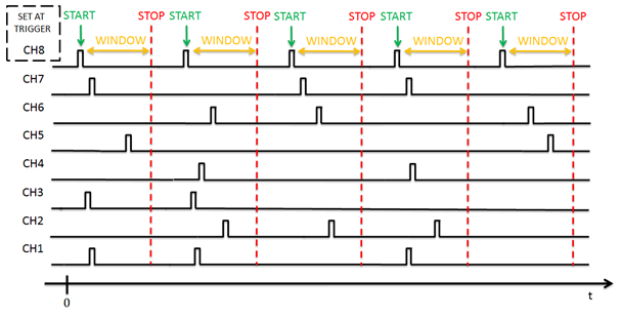

Fig. 7. Timing diagram of an acquisition. In correspondence to each START event on the trigger channel (e.g. CH8), the time intervals between START and the events detected by the ACDC into the acceptance WINDOW are calculated by the WUA-TDL-TDC.

IV. Detection of the Photon Timing in a Weak Optical Pulse

As first experiment, we make the statistic of the arrival times of the photons from a weak laser pulse with the purpose of measuring the time resolution of our complete system. High time resolution at the single photon level is of fundamental importance for analyzing fast photon emission dynamics at low illumination fluxes or in the presence of quantum emitters. An application example is the measurement with high contrast two-photon quantum interference. In LIDAR and optical time-domain reflectometry, distances are determined by the time-of-flight measurement of optical signals reflected by the target. In this case, the accuracy of the distance measurement is directly determined by the time resolution of the measurement.

The laser source used in our experiment is a Ti:Sapphire laser with 76MHz repetition rate, 6ps pulse width, and 750nm wavelength (Fig. 8). Referring to the layout shown in Fig. 4, the WUA-TDL-TDC measures the temporal distances of the events on the channel from the reference trigger on channel eight, which is given by the internal fast photodiode of the laser. The time interval and its temporal statistics from two generic channel can be shown on the host PC via the read-out software (Fig. 9). The timing measurement between two SNSPDs i and j achieve a precision (σ_{ij}) below 30ps r.m.s. (which means <23.1ps r.m.s. per channel) with a stocastical rate from 50kHz to 1.8MHz. It should be considered that the variance of the measurement σ^2_{ij} is the sum of variances of channels i and j respectively, which means that the resolution of a single channel (σ_{CH}) can be estimated to be $\sigma_{ij}/\sqrt{2}$, i.e.

$$\sigma^2_{CH} = \sigma^2_{SNSPD} + \sigma^2_{AMPLI} + \sigma^2_{CMP} + \sigma^2_{TDC} \approx$$
$$\approx (23.1ps\ r.m.s)^2$$

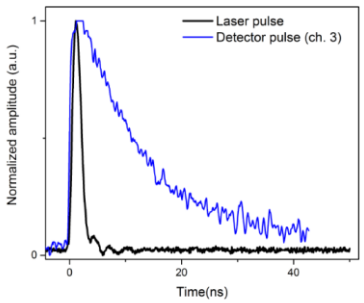

Fig. 8. Laser pulse (black) and a typical detector pulse (blue).

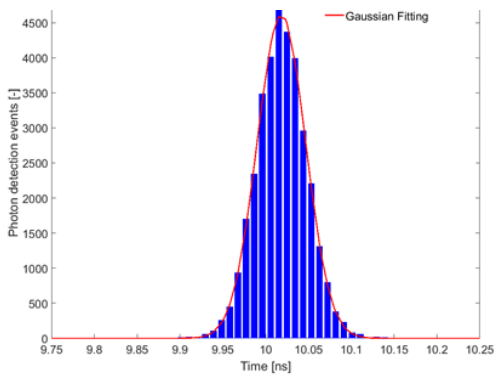

Fig. 9. Histogram of measurements of the time interval limited by a START event on Channel 2 and a STOP one on Channel 5 performed

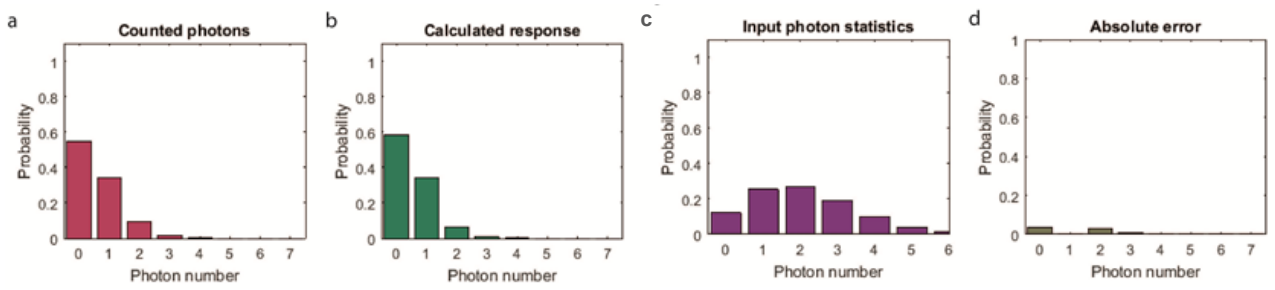

Fig. 10. (a) Detected photon probability (b) Calculated photon probability by calibrating the detection efficiency and fiber transmission loss of each channels (c) Input photon statistics adjusted by varying the input optical power, in this case the average photon number is 2.11 photons/pulse. (d) Absolute error between the measurement shown in (a) and the calculated response of (b).

V. Detection of the Photon Statistics in a Weak Optical Pulse

Thanks to the ACDC part, we measure the number of photons in weak optical pulses by measuring the photon statistics. Photon number resolution in the few-photon regime is a crucial feature for the development of quantum information technologies like quantum cryptography.

Since the absorption of more than one photon simultaneously in a SNSPD gives the same electrical output as if one photon is absorbed, a single SNSPD cannot distinguish the precise number of photon hitting the detector. In our experiments, we overcome this limitation by spatially multiplexing the optical signal onto 7 different SNSPDs installed in a cryostat based on a Gifford-McMahon closed-cycle cryo-cooler and making the photon statistic by means of the ACDC implemented in the PL part of the SoC (Fig. 4).

Other ways to measure the photon number in a weak optical pulse are to use parallel detectors to output electrical pulses of different height as a function of the number of detectors transitioning to the normal state [5, 6]. This technique requires the detectors to be operated at a much lower current than the critical current, thereby operating them below the optimum efficiency point. Alternatively, one can apply schemes for time multiplexing of the photons [5, 6]. An incident pulse is split into N weaker pulses which are delayed compared to each other by a series of fiber delay-lines. If sufficiently long fibers are used, in order to delay the photons for a value longer than the detector dead time, this architecture enables for measuring photon statistics using a limited number of photon detectors. However, this implementation is not easily scalable for high photon number and it is not suitable for high repetition rates, i.e. high photon fluxes.

First, we measured the eight transmission coefficients of the splitter and the total detection efficiency using the not attenuated and non-pulsed beam at 466nW by means of a calibrated optical power meter.

The evidence was that the fiber multiplexer presents substantial losses, overall around 30% (Tab. II), due to reflections at the fiber-air interface. The superconducting detectors are optimized for highest efficiency at 800 nm by tuning the width of an optical cavity during the fabrication process, which results in detection efficiencies up to 80.7%.

As a consequence of the detection efficiency, the fiber was connected to the fiber multiplexer towards the detectors.

Each detection channel as well as the transmission of each fiber has been separately calibrated. The efficiency is measured with a 125nW continuous optical power with 60dB attenuation.

The number of dark counts is about 50 count per second per channel. The detector efficiency takes into account the losses of an optical fiber inside the cryostat where the detectors are mounted, whereas the system efficiency takes into account both the detector efficiency and the losses of the fiber multiplexer.

This efficiency has been used, for each input power, to calculate the expected response of the measurement setup and thus to reconstruct the precise average number of photons in the optical pulse arriving at the fiber splitter (Tab. II).

These results show that we can measure the exact average number of photons with an optical pulse in the few photon regime that is a skill fundamental in quantum computing and quantum cryptography.

For instance, the calculated response for the case of 2.11

Table II.
Results of the Calibration Procedure Run for Each Channel

Detector channel	Detector eff. [%]	Fiber eff. [%]	System eff. [%]
Channel 1	47.6%	9.0%	4.3%
Channel 2	71.1%	11.5%	8.2%
Channel 3	80.7%	10.5%	8.5%
Channel 4	37.7%	8.2%	3.1%
Channel 5	51.3%	6.9%	3.5%
Channel 6	37.6%	6.2%	2.3%
Channel 7	65.3%	8.4%	5.5%

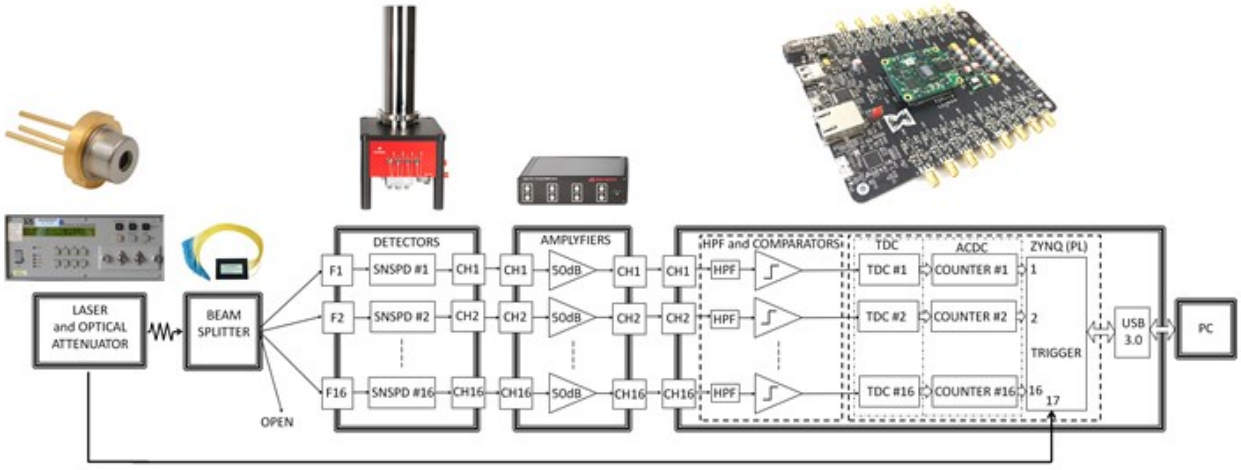

Fig. 11. Block diagram of the experimental setup extended to 16 channels.

photons/pulse is reported in Fig. 10c, along with a comparison with the measured results presented in Fig. 10a. The calculation of the system response accounts for the probability that two photons hit the same detector during the same measurement window.

There is very good agreement between experimental result and calculated response, achieving relative error <10%. At low optical fluxes, i.e. average photon number <<1, the error increases because of the ratio between dark counts and detection events. At average photon number higher than 4, the error increases due to the limited amount of detectors in the experiment.

VI. IMPROVEMENTS

Our approach makes use of a scalable WUA-TDL-TDC/ACDC architecture that is connected to several high efficiency photon detectors. This architecture can be readily scaled up to 16 ÷ 32 detection channels thanks to the use of FPGA parallel architecture without compromising the showed performance. The device can make full use of the superconducting nanowire performance of photon detection and time resolution. A new experiment at 16 channels is in progress (Fig. 11)

CONCLUSIONS

An 8-channel TDC/ACDC system for readout from SNSPDs has been presented and utilized for counting photons in weak optical pulses using superconducting single photon detectors. A proper circuit based on programmable threshold comparator and high-pass filter is used for making digital the amplified analog pulsed produced by the photon excitation of SNSPDs. The proposed system by means of the TDC make possible to measure, with a total precision less than 23.1ps r.m.s., the photon timing detections and, through the ACDC, the computing of the photon statist. The TDC/ACDC system are totally implemented in the Programmable Logic of a SoC. This work was used as a case study for extend the system at 16 channels thanks to the use of FPGA/SoC parallel architecture. The 16-channel TDC architecture has been realized and it is currently implemented in combination with 16 superconducting single photon detectors is forthcoming. Thanks to the increased number of acquisition channels, more complex quantum optical measurements will be enabled.

REFERENCES

[1] Peter A. Morris et al., Imaging with a small number of photons. Nature Communicat 6, Article number: 5913 doi:10.1038/ncomms6913

[2] N. Gisin, Quantum Cryptography, Rev. Mod. Phys. 74, 145 – (2002)

[3] IE Zadeh et al., Single-photon detectors combining high efficiency, high detection rates, and ultra-high timing resolution, APL Photonics 2, 111301 (2017).

[4] N. Lusardi, F. Garzetti, G. Bulgarini, R.B.M. Gourgues, J.W.N. Los, A. Geraci, “Single Photon Counting through Multi-channel TDC in Programmable Logic”, Proc. of the 2016 IEEE Nuclear Science Symposium, October 29-November 5, 2016, Strasbourg, FRA.

[5] N. Lusardi, A. Geraci, R. B. M. Gourgues, J. W.N. Los, G. Bulgarini, “Array of Superconducting Nanowire Single Photon Detectors Resolving the Number of Photons in a Weak Optical Pulse", Proc. of the 2016 IEEE Nuclear Science Symposium, October 29-November 5, 2016, Strasbourg, FRA.

[6] N. Lusardi, J. W. N. Los, R. B. M. Gourgues, G. Bulgarini, and A. Geraci, “Photon counting with photon number resolution through superconducting nanowires coupled to a multi-channel TDC in FPGA”, RSI – Review of Sceintific Instruments, Volume 88, Issue 3, March 2017.

[7] Xilinx, 2012, 14.2 Version, Zynq Architecture. Online available: http://www.ioe.nchu.edu.tw/Pic/CourseItem/4468_20_Zynq_Architecture.pdf.

[8] http://www.analog.com/en/products/digital-to-analog-converters/ad5671r.html

[9] http://www.analog.com/media/en/technical-documentation/data-sheets/ADCMP604_605.pdf

[10] N. Lusardi, A. Geraci, "Eight-Channels High-Resolution TDC in FPGA", Proc. of the 2015 IEEE Nuclear Science Symposium, October 31-November 7, 2015, San Diego, USA.

[11] N. Lusardi, A. Geraci, "Comparison of Interpolation Techniques for TDCs Implementation in FPGA", Proc. of the 2015 IEEE Nuclear Science Symposium, October 31-November 7, 2015, San Diego, USA.